Inductor Winding Capacitance Cancellation Using Mutual Capacitance Concept for Noise Reduction Application

Shuo Wang, *Member, IEEE*, Fred. C. Lee, *Fellow, IEEE*, and Jacobus Daniel van Wyk, *Fellow, IEEE*

***Abstract*—In this paper, the properties of mutual capacitance between two capacitors are first discussed. It is found that the effects of mutual capacitance can be represented by two positive or negative capacitors across the two capacitors. These two equivalent capacitors can be used to cancel the parasitic capacitance of inductors. Because the mutual capacitance can be emulated using two small capacitors, the proposed method can easily be implemented in practical components. The prototypes are then built and the cancellation is verified using a network analyzer. Further EMI measurements in a practical power circuit prove that there is a significant improvement in the inductor's filtering performance.**

***Index Terms*—Electromagnetic interference (EMI) filter, mutual capacitance, winding capacitance, winding capacitance cancellation.**

I. Introduction

An inductor is a very important filter component for electromagnetic interference (EMI) noise suppresses because its impedance increases as frequency increases. However, the inductor's operation frequency range is limited because of the parasitic capacitance. The turn-to-turn capacitance and turn-to-core capacitance make an inductor more like a capacitor at high frequencies [5]. When an inductor model is considered, the parasitic capacitance is usually lumped together as an equivalent parallel capacitance (EPC), which is parallel to the inductor's inductance L. The winding loss and core loss are usually lumped together as an equivalent parallel resistance (EPR), which is parallel to the inductance L. Fig. 1 shows a simple model for the inductor. Fig. 2 shows the typical impedance curves for two practical inductors.

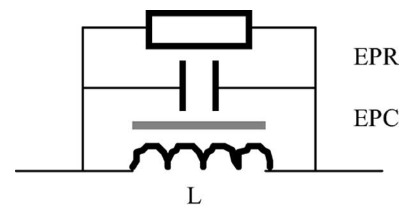

Fig. 1. Equivalent circuit for a practical inductor.

In Fig. 2, the inductance determines the impedances of the inductors at low frequencies, and the EPC determines the impedances of the inductors at high frequencies. For curve 1, the quality factor Q is larger than one, so EPC_1 and L_1 resonate at $f_1 = 1/(2\pi\sqrt{L_1 \times \mathrm{EPC}_1})$. The highest impedance is equal to EPR_1 and it happens at f_1. For curve 2, because the quality factor is smaller than one, the first corner frequency is determined by EPR_2 and L_2 as $f_3 = \mathrm{EPR}_2/2\pi L_2$. The second-corner frequency is determined by EPR_2 and EPC_2 as $f_4 = 1/(2\pi \times \mathrm{EPR}_2 \times \mathrm{EPC}_2)$. The highest impedance is equal to EPR_2 and it happens at $f_2 = 1/(2\pi\sqrt{L_2 \times \mathrm{EPC}_2})$. Based on this analysis, the highest impedance an inductor can achieve is EPR; however, because of EPC, the impedance is much smaller than EPR at high frequencies. If the EPC is zero, then the impedance of an inductor at high frequencies is EPR, which is good for noise attenuation at high frequencies.

In power electronics systems, the conducted EMI spectrum ranges from the switching frequency to 30 MHz. EMI standards specify the frequency range and noise limit, which switching mode power electronics systems need to meet. EMI filters are needed to attenuate the noise to satisfy the EMI standards. A typical low-pass differential mode (DM) EMI filter for a power electronics application is shown in Fig. 3. There are two equal inductors (L_1 and L_2) on each line and two capacitors, C_1 and C_2, across two lines. Two inductors can be coupled to save size and cost. At frequencies higher than the self resonant frequencies of the inductors, the inductors perform like capacitors, and therefore, the filter is no longer the expected lowpass filter.

This paper introduces a method employing a mutual capacitance concept to cancel the EPC of inductors. Prototypes are built with the proposed method. Small signal measurements are first carried out to verify the proposed method. The prototypes are then used in practical power electronics circuits for conducted EMI measurement (with large current bias and excitation). Both the small signal and practical EMI measurement prove that there is a significant improvement on the inductor's filtering performance.

II. Winding Capacitance Cancellation Using Mutual Capacitance Concept

The mutual capacitance concept has evolved from the duality principle in [1] to the correspondent part of the mutual inductance. The basic properties of mutual capacitance are derived and a physical model using a simple parallel plate capacitor is demonstrated in [1]. This paper will further derive the properties for winding capacitance cancellation.

Manuscript received November 22, 2005; revised January 10, 2006.

The authors are with the National Science Foundation Engineering Research Center for Power Electronics Systems, the Bradley Department of Electrical and Computer Engineering, Virginia Polytechnic Institute and State University (Virginia Tech), Blacksburg, VA 24061 USA.

Digital Object Identifier 10.1109/TEMC.2006.873867

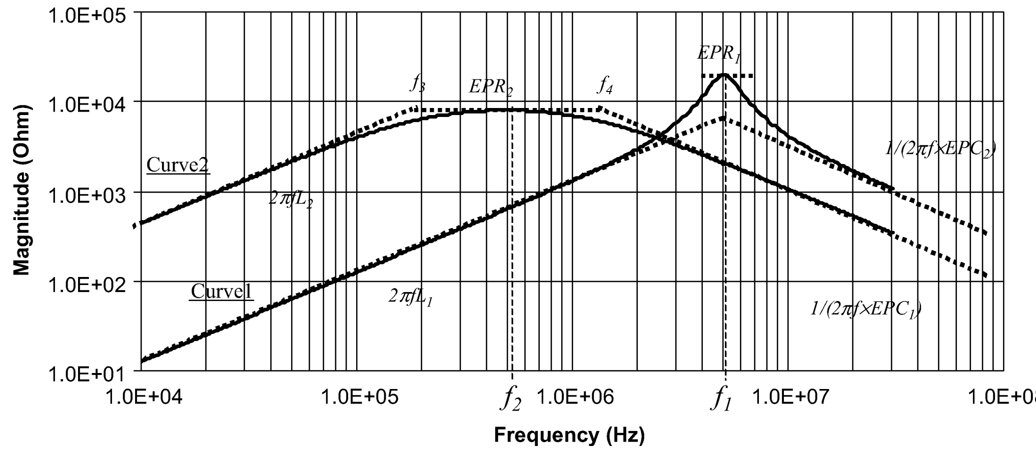

Fig. 2. Impedances of two inductors.

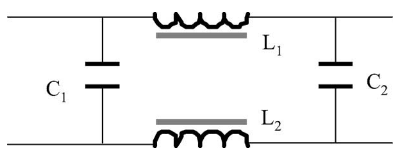

Fig. 3. Differential mode EMI Filter.

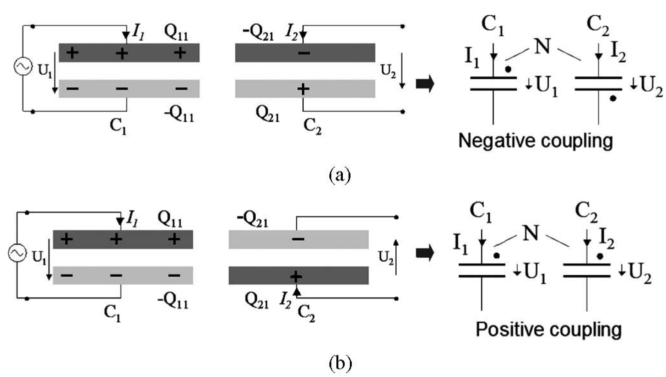

Fig. 4. Mutual capacitance between two parallel-plate capacitors. (a) Negative coupling. (b) Positive coupling.

Fig. 4 shows two parallel-plate capacitors that are physically close to each other. Two capacitors have the same voltage reference direction, as seen in Fig. 4(a), and opposite voltage reference direction as seen in Fig. 4(b). An external voltage source is added to C_1. The positive charge Q_{11} is then built on the upper plate and the negative charge $-Q_{11}$ is built on the lower plate. As a result, the negative charge $-Q_{21}$ is induced on the upper plate of C_2, and the positive charge Q_{21} is induced on the lower plate of C_2. Due to the different voltage reference direction relationship in Fig. 4(a) and (b), the mutual capacitance N can be positive or negative. The mutual capacitance is defined similarly to the mutual inductance as

$$N = \frac{Q_{21}}{U_1}. \tag{1}$$

Considering a general case, for negative coupling, the following relationship is satisfied:

$$I_1 = j\omega C_1 U_1 - j\omega N U_2 \tag{2}$$

$$I_2 = -j\omega N U_1 + j\omega C_2 U_2. \tag{3}$$

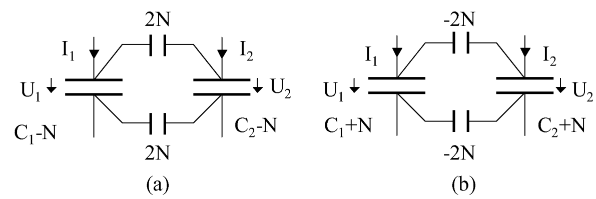

Fig. 5. Equivalence for mutual capacitance between two capacitors. (a) Negative coupling. (b) Positive coupling.

For positive coupling, the following relationship holds:

$$I_1 = j\omega C_1 U_1 + j\omega N U_2 \tag{4}$$

$$I_2 = j\omega N U_1 + j\omega C_2 U_2. \tag{5}$$

Equations (2) and (3) can further be expressed as

$$I_1 = j\omega (C_1 - N) U_1 + j\omega N (U_1 - U_2) \tag{6}$$

$$I_2 = j\omega N (U_2 - U_1) + j\omega (C_2 - N) U_2 \tag{7}$$

and (5) and (6) can be further expressed as

$$I_1 = j\omega (C_1 + N) U_1 - j\omega N (U_1 - U_2) \tag{8}$$

$$I_2 = -j\omega N (U_2 - U_1) + j\omega (C_2 + N) U_2. \tag{9}$$

From (6) and (7), Fig. 4(a) can be equivalent to Fig. 5(a). From (8) and (9), Fig. 4(b) can be equivalent to Fig. 5(b).

In Fig. 5(a), the negative coupling between two capacitors can be represented by showing two extra capacitors with a capacitance $2N$ across the two plates of two capacitors with the same polarity. At the same time, the capacitance of each capacitor is reduced by N. In Fig. 5(b), similarly, the positive coupling between two capacitors can be represented by showing two extra capacitors with a capacitance $-2N$ across the two plates of two capacitors with the same polarity. The capacitance of each capacitor is increased by N.

Based on this analysis, if C_1 and C_2 in Fig. 3 have a positive mutual capacitance N, which is equal to the half of the winding capacitance of the inductors, the winding capacitance of inductors are canceled, since $-2N$ is in parallel with the positive winding capacitance. On the other hand, when the winding capacitance of L_1 and L_2 is negative (will be discussed later),

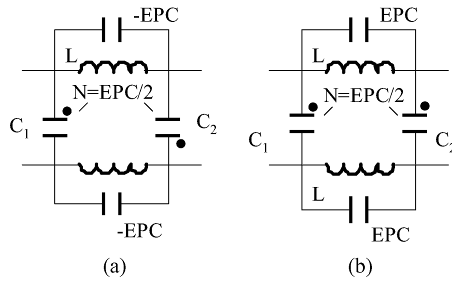

Fig. 6. Cancellation of winding capacitance using mutual capacitance between two capacitors. (a) Canceling negative winding capacitance −EPC. (b) Canceling positive winding capacitance +EPC.

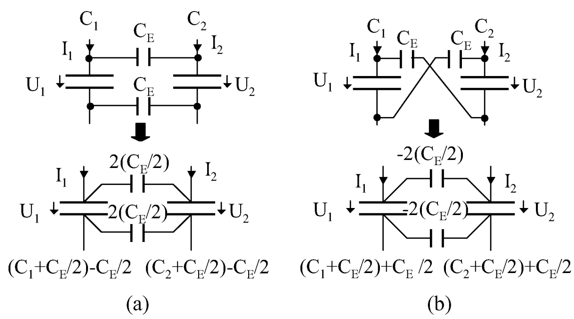

Fig. 7. Using two small capacitors C_E to emulate the mutual capacitance. (a) Emulating negative coupling. (b) Emulating positive coupling.

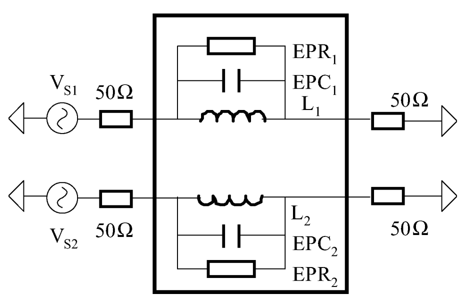

Fig. 8. Measurement setup using Agilent E5070B.

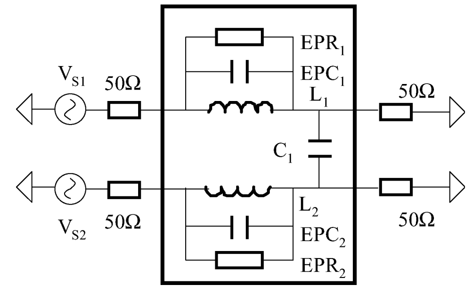

Fig. 9. Measurement setup using Agilent E5070B.

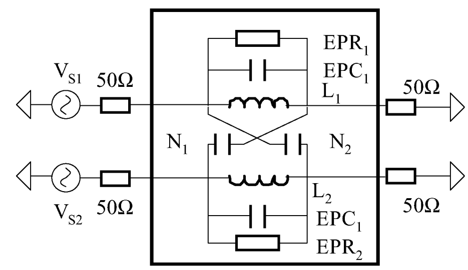

Fig. 10. Measurement setup using Agilent E5070B.

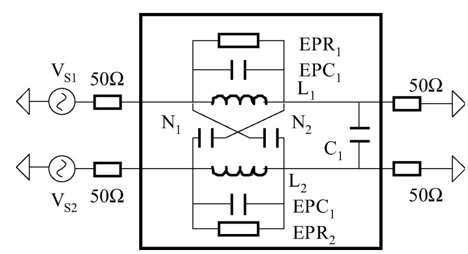

Fig. 11. Measurement setup using Agilent E5070B.

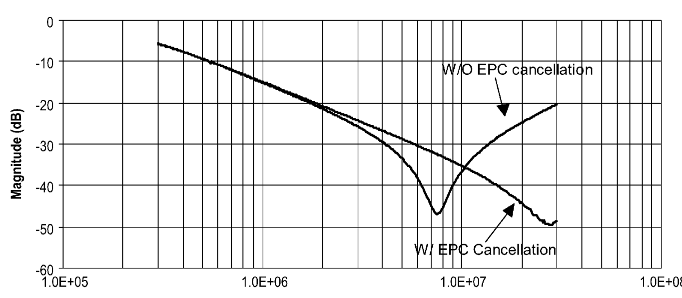

Fig. 12. Improvement of inductor filtering performance at high frequencies due to the EPC cancellation.

then if C_1 and C_2 have a negative mutual capacitance N, which is equal to the half of the winding capacitance of the inductors, the winding capacitance of inductors is canceled since $2N$ capacitance is in parallel with the negative winding capacitance (Fig. 6).

The design of mutual capacitance between two capacitors seems difficult for existing commercial discrete capacitors. Fortunately, the mutual capacitance can easily be emulated using two extra small capacitors (Fig. 7).

In Fig. 7, two extra capacitors with the capacitance of C_E are used to emulate the mutual capacitance $C_E/2$ between capacitors with capacitance $(C_1 + C_E)/2$ and $(C_2 + C_E)/2$. C_1 and C_2 are actually not necessary for winding capacitance cancellation, so only two small capacitors are enough. The mutual capacitance cancellation is then easily realized by using two small capacitors with the same capacitance as the winding capacitance.

Compared with the common practice in practical EMI filter design, by applying the proposed technique, the filter would have better high-frequency performance, smaller size, and lower cost because the winding capacitance is canceled. For the common practice, a larger core is usually used to reduce winding capacitance. However, the filter size is larger and improvement is still limited. Another common practice is using one more stage EMI filter to get more attenuation at higher cost and larger size. In both cases, the filter is not as efficient as the filter with winding-capacitance cancellation.

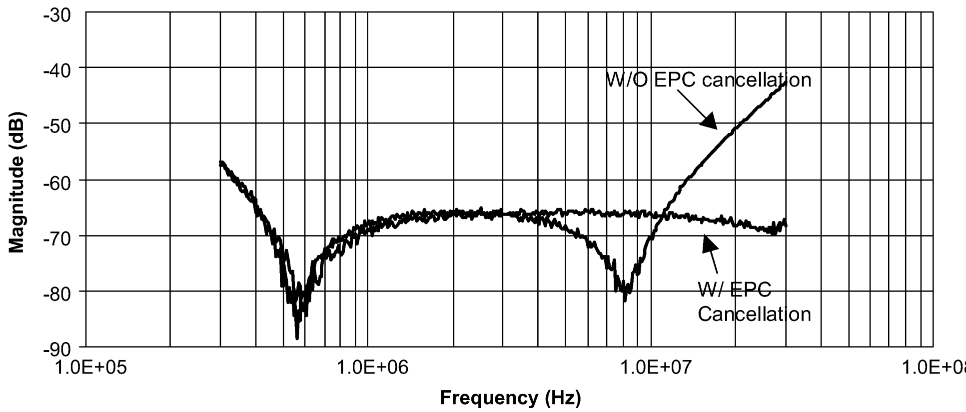

Fig. 13. Improvement of filter performance at high frequencies due to the EPC cancellation.

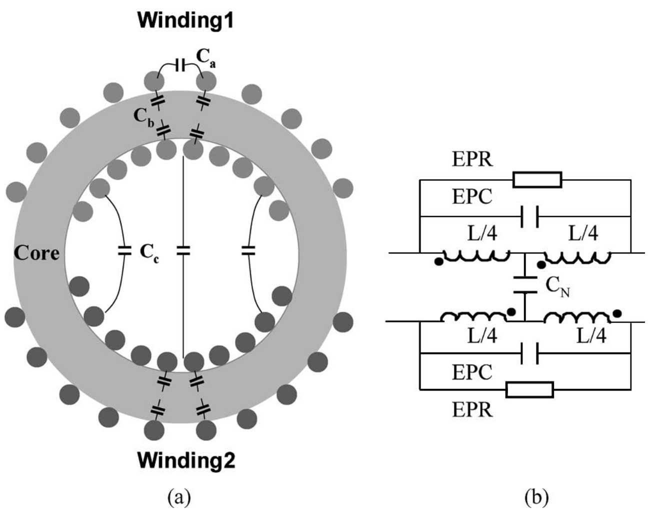

Fig. 14. Parasitic capacitance between two inductor windings. (a) Inductor structure. (b) Equivalent circuit.

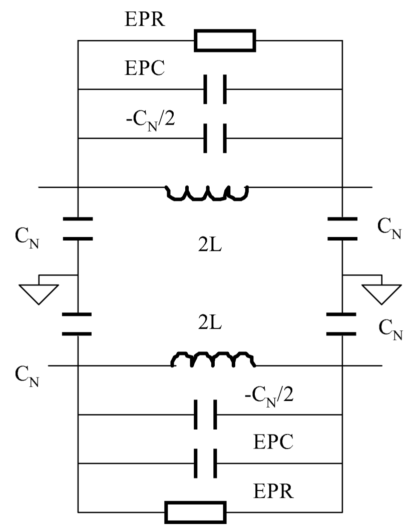

Fig. 15. Equivalent circuit for coupled inductors.

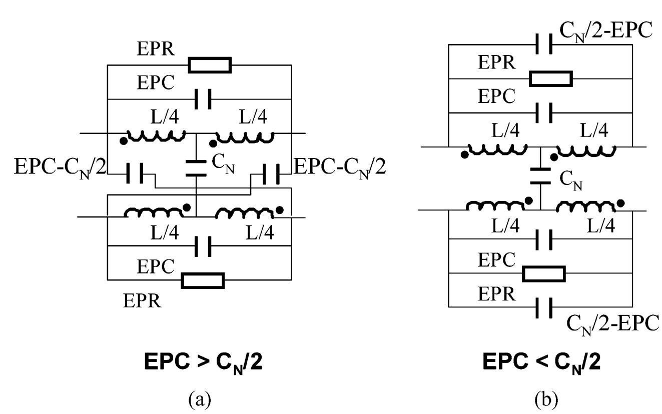

Fig. 16. Winding capacitance cancellation strategy. (a) $\mathrm{EPC} > \mathrm{C_N}/2$. (b) $\mathrm{EPC} < \mathrm{C_N}/2$.

III. Experiments

Four experiments are carried out to implement and verify the proposed method. An Agilent E5070B, four-port balanced ENA RF network analyzer is used in the experiments. The frequency is swept from 300 kHz to 30 MHz. In the first two experiments, two inductors are not coupled. The SDD21 of the filter with only two inductors is first measured as shown in Fig. 8. The self-parasitics for two inductors are $L_1 = 42.34\ \mu$H, $\mathrm{EPC}_1 = 10.3$ pF, $\mathrm{EPR}_1 = 10.87$ kΩ, $L_2 = 42.44\ \mu$H, $\mathrm{EPC}_2 = 11.13$ pF, and $\mathrm{EPR}_2 = 10.67$ kΩ. An L-type EMI filter is then built using one capacitor ($C = 3.22\ \mu$F, $\mathrm{ESL} = 20.9$ nH, $\mathrm{ESR} = 13.6$ mΩ) and these two inductors. The SDD21 of this filter is also measured, as shown in Fig. 9.

In the second experiment, the proposed method is applied to two inductors and the SDD21 of the filter with only these two EPC-canceled inductors is measured as shown in Fig. 10. The capacitance of two cancellation capacitors is $N_1 = 9.99$ pF and $N_2 = 10.24$ pF, which are a little bit smaller than EPC_1 and EPC_2. An L-type EMI filter is then built using these two EPC-canceled inductors and the same capacitor as used in the first experiment. The SDD21 of this filter is also measured as shown in Fig. 11. The measurement results are compared in Figs. 12 and 13.

In Fig. 12, the SDD21 of the original inductor has a parallel resonance due to the EPC around 7.5 MHz, which makes the inductor performance worse above 10 MHz. After EPC is canceled, the resonance moves to around 28 MHz, which means EPC is reduced by 93%. As a result, the filter's performance improves much above 10 MHz, as shown in Fig. 13. At 30 MHz,

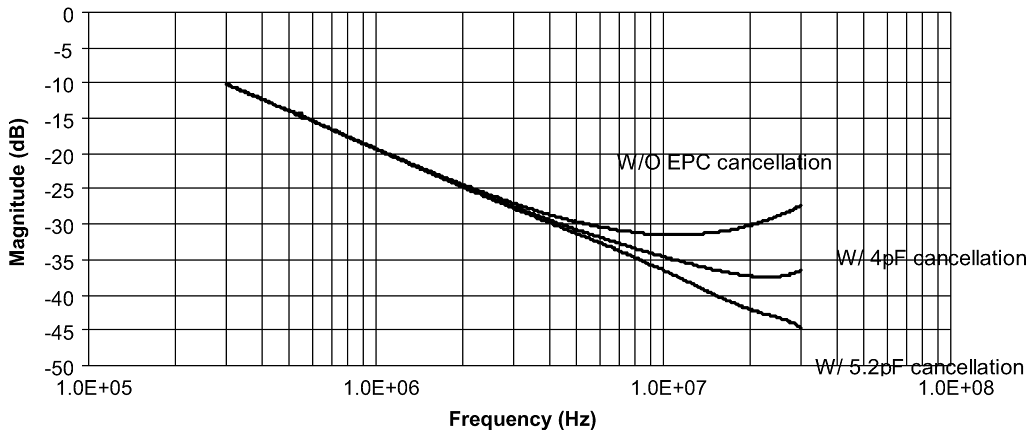

Fig. 17. Improvement of inductor filtering performance at high frequencies due to the EPC cancellation.

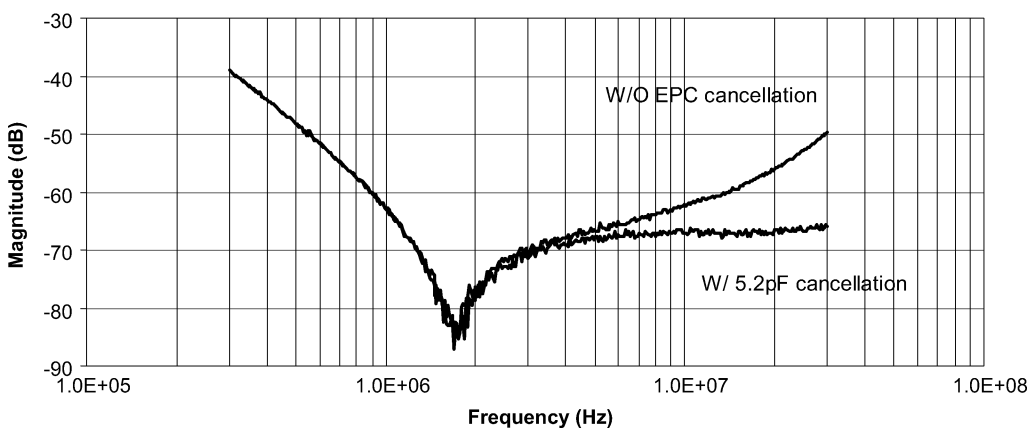

Fig. 18. Improvement of filter performance at high frequencies due to the EPC cancellation.

the SDD21 of the EMI filter with canceled EPC has about a 26-dB (a factor of 200) improvement. The dips around 670 kHz in Fig. 13 are caused by the series resonance of C_1.

When two inductors are coupled, since two inductors are located on one core, the effects of the parasitic capacitance between two windings cannot be ignored. This will make the inductor-winding capacitance different from the separated inductor case. Fig. 14 shows a toroidal inductor with two coupled windings.

In Fig. 14, it is assumed that two windings are exactly same, so that all parameters are same. It is also assumed that the coupling coefficient between two windings is a unit and that the inductance for one winding is L. In Fig. 14(a), there are three kinds of parasitic capacitance in the inductor: turn-to-turn capacitance $C_{\rm a}$, turn-to-core capacitance $C_{\rm b}$, and winding-to-winding capacitance $C_{\rm c}$ [6]. Their effects can be represented by EPC and $C_{\rm N}$ in Fig. 14(b). EPC represents the effects of $C_{\rm a}$ and $C_{\rm b}$. $C_{\rm N}$ represents the effects of $C_{\rm c}$ and $C_{\rm b}$, i.e., the parasitic capacitance between two windings. Fig. 14(b) is inductively decoupled and is equivalent to Fig. 15 using the network theory [2].

In Fig. 15, if EPC $> C_{\rm N}/2$, then the equivalent winding capacitance is positive. The parallel resonant frequency is given by (10). To cancel it, two capacitors with the value of EPC—$(C_{\rm N}/2)$ need to be diagonally connected, as shown in Fig. 16(a). If EPC $< C_{\rm N}/2$, then the equivalent winding capacitance is negative. There will be no resonance but minimum impedance because the negative capacitance is inductive. The frequency for the minimum impedance is given by (11). To cancel it, two capacitors with the value of $(C_{\rm N}/2)$–EPC need to be parallel with the windings, as shown in Fig. 16(b). It finally turns out that to cancel the negative equivalent winding capacitance, more capacitance needs to be paralleled with two windings.

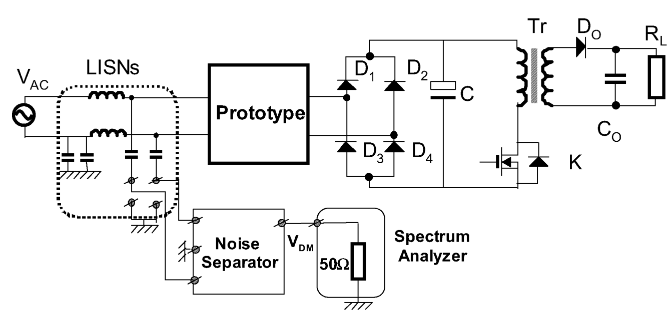

Fig. 19. EMI measurement for the prototypes in a practical power converter.

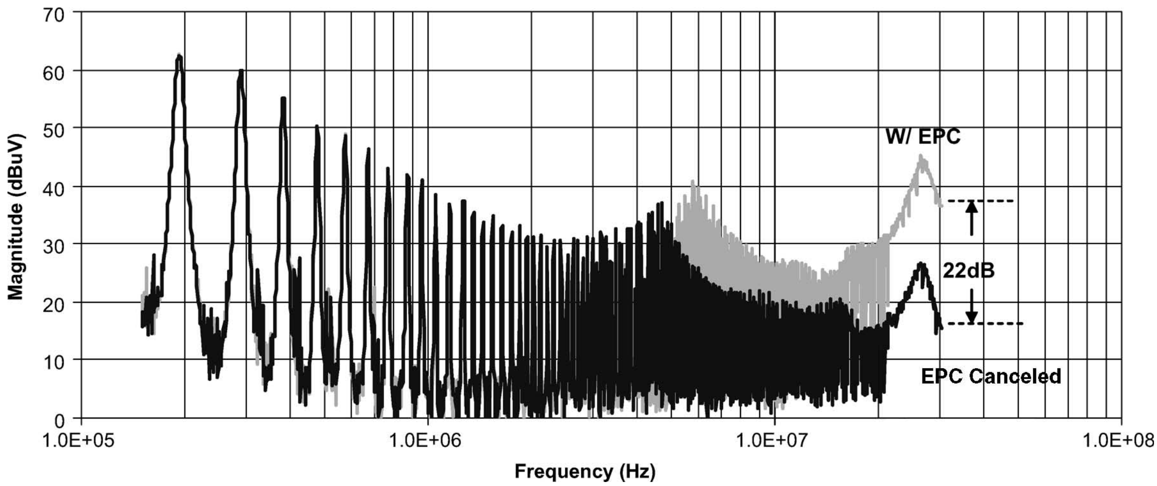

Fig. 20. EMI noise reduction with winding capacitance cancellation technique.

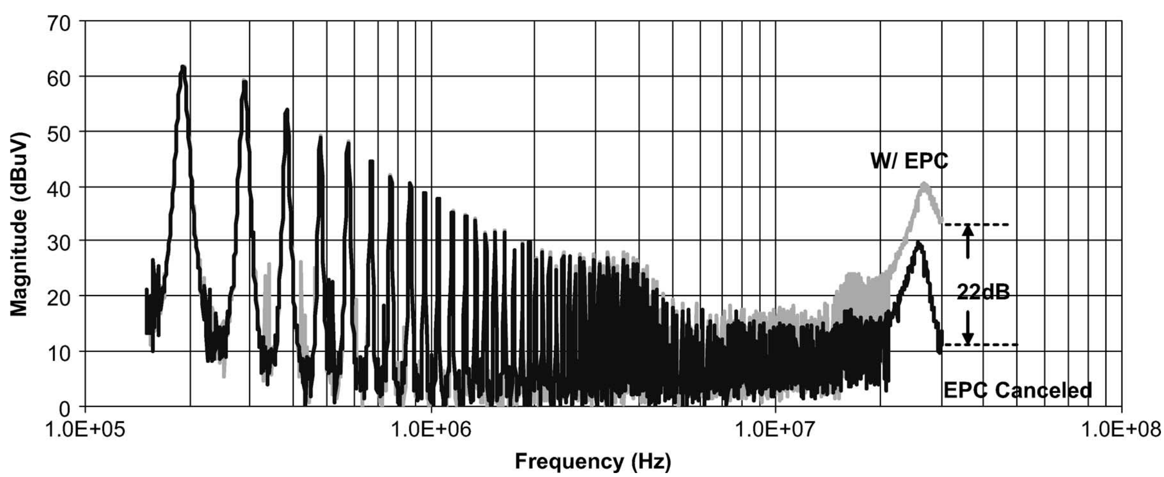

Fig. 21. EMI noise reduction with winding capacitance cancellation technique.

These two concepts for positive and negative winding capacitance cancellations correspond to the positive and negative couplings in Fig. 7. The following can be used to determine C_N via SDD21 measurement:

$$f_1 = \frac{1}{2\pi\sqrt{2L\left(\mathrm{EPC} - \frac{C_{\mathrm{N}}}{2}\right)}} \tag{10}$$

$$f_1 = \frac{1}{2\pi\sqrt{2L\left(\frac{C_{\mathrm{N}}}{2} - \mathrm{EPC}\right)}}. \tag{11}$$

In the experiments, each winding of the coupled inductor has an inductance of 20 μH; EPC is 2.2 pF, and EPR is 3.2 kΩ. The C_{N} is 14.8 pF, which is calculated by (11) via SDD21 measurment. Because EPC $< (C_{\mathrm{N}}/2)$, then two cancellation capacitors with a capacitance of 5.2 pF each need to be parallel with two windings to cancel the equivalent winding capacitance -5.2 pF. Fig. 17 shows the measured SDD21s for the inductor with and without EPC cancellation. An L-type EMI filter is also built using one capacitor ($C = 477$ nF, ESL $= 18.5$ nH, ESR $= 35.4$ mΩ) and the coupled inductors. The SDD21 of this filter with or without EPC cancellation is measured and shown in Fig. 18.

In Fig. 17, three SDD21s, the original SDD21, the SDD21 with 4-pF cancellation, and the SDD21 with 5.2-pF cancellation were measured. It is shown that after two 5.2-pF capacitors are paralleled with the two windings, respectively, the inductor got the best performance above 5 MHz because the equivalent winding capacitance is almost canceled. As a result, the EMI filter response is almost flat above 5 MHz. For the original case without EPC cancellation, the filter performance is worse above 5 MHz, due to the negative equivalent capacitance. The performance is therefore greatly improved above 5 MHz using proposed EPC cancellation method.

The proposed technique can also be applied to a common mode EMI filter if a ground inductor is allowed in applications.

One of the practical issues to apply this proposed technique into filter production might be the implementation of cancellation capacitor, because its capacitance should be as close to winding capacitance as possible. One solution is to use a discrete capacitor parallel with a small PCB capacitor, which is a parallel-plate capacitor, composed of two pieces of copper on the top and bottom layers of the PCB. Its capacitance is tuned by changing the plate areas so that the total capacitance is close to winding capacitance. For massive production, the capacitance of the cancellation capacitor can be customized according the winding capacitance of the inductor, and therefore, no PCB capacitor is needed.

IV. EMI Measurement

Because all the experiments in Section III are under small signal excitation and of 50 Ω source and load conditions, it is necessary to make sure that the EPC cancellation still gives satisfying results with a large signal excitation, current bias, and practical source and load, especially for a power electronics application. The inductors without EPC cancellation in Figs. 12 and 17 are first connected to power lines and a practical flyback power converter in Fig. 19. The switching frequency of the power converter is 97 kHz and its harmonics extend to 30 MHz.

In Fig. 19, to measure the DM noise, two line-impedance-stabilizing networks (LISNs) are connected to power lines and the inductors. A noise separator [3] is used to provide 50-Ω load impedance for the LISNs and, at the same time, separate the DM noise from CM noise. The EMC analyzer, Agilent E7402A, is connected to the noise separator for EMI spectrum measurement. A DM noise was then measured and the data were stored.

In the second step, the EPC-canceled inductors in Figs. 12 and 17 are then connected to the circuit for EMI noise measurement. The data were also stored. Finally, the stored noise data are compared in Figs. 20 and 21. In Fig. 20, for the noncoupled inductors, the measured EMI noise after EPC is canceled is much lower than that without EPC cancellation above 5 MHz. At 30 MHz, a 22-dB improvement is achieved. In Fig. 21, for the coupled inductor, the measured EMI noise after EPC is canceled is much lower than that without EPC cancellation above 6 MHz. At 30 MHz, a 22-dB improvement is achieved. These two experiments show that the proposed method works in practical circuits, even with a larger signal excitation, current bias, and non-50-Ω source and load impedances.

V. Conclusion

The theory and design of using a mutual capacitance concept to cancel the effects of parasitic capacitance of inductors is discussed in this paper. The prototypes are first verified by the measurement using a 50-Ω-based network analyzer and then verified by the EMI measurements in a practical power converter. The measurements show that the proposed method can efficiently improve the inductor's filtering performance beyond its self resonant frequency. By applying the proposed technique, an EMI filter design with good high-frequency performance, small size, and low cost is therefore possible.

References

[1] Z.-L. Liang, "Mutual capacitance-duality principle evolved from planar network," *IEEE Trans. Circuits Syst. I: Fundam. Theory Appl.*, vol. 39, no. 12, pp. 1005–1006, Dec. 1992.

[2] R. Chen, J. D. van Wyk, S. Wang, and W. G. Odendaal, "Improving the characteristics of integrated EMI filters by embeded conductive layers," *IEEE Trans. Power Electron.*, vol. 20, no. 3, pp. 611–619, May 2004.

[3] S. Wang, F. C. Lee, and W. G. Odendaal, "Characterization, Evaluation and design of noise separator for conducted EMI noise diagnosis," *IEEE Trans. Power Electron.*, vol. 20, no. 4, pp. 974–982, Jul. 2004.

[4] *Agilent E5070B/E5071B ENA Series RF Network Analyzers User's Guide*: 5th ed., Agilent Technologies, 2004.

[5] A. Massarini and M. K. Kazimierczuk, "Self-capacitance of inductors," *IEEE Trans. Power Electron.*, vol. 12, no. 4, pp. 671–676, Jul. 1997.

[6] A. Baccigalupi, P. Daponte, and D. Grimaldi, "On a circuit theory approach to evaluate the stray capacitances of two coupled inductors," *IEEE Trans. Instrum. Meas.*, vol. 43, no. 5, pp. 774–776, Oct. 1994.

Shuo Wang (S'03–M'06) received the B.S.E.E. degree from the Southwest Jiaotong University, Chengdu, China, in 1994, the M.S.E.E. degree from the Zhejiang University, Hangzhou, China, in 1997, and the Ph.D. degree from the Center for Power Electronics Systems (CPES), Virginia Polytechnic Institute and State University (Virginia Tech), Blacksburg, in 2005.

From 1997 to 1999, he was with ZTE Telecommunication Corporation, Shenzhen, China, where he was a Senior R&D Engineer and was responsible for the development and support of the power supply for wireless products. In 2000, he worked at UTstarcom Telecommunication Corporation, Hangzhou, where he was responsible for the development and support of the optical access networks. Since 2005, he has been a Research Assistant Professor at the CPES. He holds one US patent.

Dr. Wang has served an Associate Editor for the Power Electronics Devices and Components Committee of IEEE Transactions on Industry Applications since 2005. He is also the co-recipient of William M. Portnoy Award for a paper published in IEEE IAS Annual Conference in 2004.

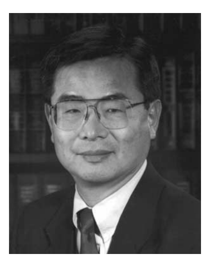

Fred C. Lee (S'72–M'74–SM'87–F'90) received the B.S. degree from the National Cheng Kung University, Tainan City, Taiwan, R.O.C., in 1968 and the M.S. and Ph.D. degrees from Duke University, Durham, NC, in 1972 and 1974, respectively, all in electrical engineering.

He is currently a University Distinguished Professor at Virginia Polytechnic Institute and State University (Virginia Tech), Blacksburg, where he also directs the Center for Power Electronics Systems (CPES), which is a national science foundation engineering research center. He holds 30 US patents and has published over 175 journal articles in refereed journals and more than 400 technical papers in conference proceedings.

Dr. Lee is a recipient of the Society of Automotive Engineering's Ralph R. Teeter Education Award (1985), Virginia Tech's Alumni Award for Research Excellence (1990), and its College of Engineering Dean's Award for Excellence in Research (1997). In 1989, he received the William E. Newell Power Electronics Award. He is also the recipient of the Power Conversion and Intelligent Motion Award for Leadership in Power Electronics Education (1990), the Arthur E. Fury Award for Leadership and Innovation in Advancing Power Electronic Systems Technology (1998), and the IEEE Millennium Medal.

Jacobus Daniel van Wyk (F'90) received the M.Sc.Eng. degree from the University of Pretoria, Gauteng, South Africa, in 1966, the Dr. Sc. Tech. (*cum laude*) degree from the Technical University, Eindhoven, The Netherlands, in 1969, and the D.Sc. (Eng.) (*honoris causa*) degree from the University of Natal, Durban, South Africa, in 1996.

From 1961 and 1971, he has worked with the S.A. Iron and Steel Corporation, University of Pretoria, and the technical and scientific staff of the Technical University, Eindhoven. From 1971 to 1995, he was a Chaired Professor of Electrical and Electronic Engineering at the Rand Afrikaans University, Johannesburg, South Africa, holding Chairs in electronics

and in power electronics till 1992. He founded the Industrial Electronics Technology Research Group with the Faculty of Engineering in 1978 and directed this unit until 1999. Since July 1995, he has held a special University Council Research Chair in Industrial Electronics at the Rand Afrikaans University and, since 2000, in a part-time capacity. He joined the Bradley Department of Electrical and Computer Engineering, Virginia Polytechnic Institute and State University (Virginia Tech), Blacksburg, in January 2000, where he is the J. Byron Maupin Professor of Engineering. At Virginia Tech, he is with Center for Power Electronics Systems (CPES), which is a national science foundation engineering research center, where he leads the High Density Integration Research Thrust. He has worked and published in the fields of semiconductors, microelectronics, electric materials, electromechanical energy conversion, electric drives, power electronics, industrial electronics, control, alternative energy systems, electric vehicles, and many diverse applications in industry, mining, transportation, and electrical energy supply systems. His present research interest is in integrated electronic power processors.

Dr. van Wyk is a Fellow of the South African Institute of Electrical Engineers. He has served as Editor-in-Chief of the IEEE TRANSACTIONS ON POWER ELECTRONICS since 2002. He has been a recipient and co-recipient of 20 prize papers awards, including 11 IEEE prize paper awards for some of his work, and was the recipient of the prestigious IEEE William E. Newell Power Electronics Award in 1995 and an IEEE Third Millennium Medal in 2000. He is active in several capacities within the IEEE and its societies, as well as in other scientific and engineering organizations, especially regarding publishing and organization of conferences. He has received a range of other awards from IEEE Societies, as well as from the South African Institute of Electrical Engineers.